

Spin-flip scattering in ZnTe—experimental*

R. L. Hollis[†] and J. F. Scott

Department of Physics and Astrophysics, University of Colorado, Boulder, Colorado 80309

(Received 28 June 1976)

Spin-flip scattering of laser light at fields up to 148 kG in *p*-ZnTe is described. Experiments varying excitation wavelength, power, magnetic field, polarization, and sample characteristics are detailed. The observed spectral features are assigned to the spin flip of heavy holes and to electrons and holes bound to donor and acceptor levels. The energy, line-shape, and linewidth field dependence of the heavy-hole scattering are compatible with theoretical calculations. The gyromagnetic ratio of the shallowest-heavy-hole level is found to lie between $g = 0.9$ and $g = 1.1$, depending upon the sample, compatible with the theoretical value 0.92 ± 0.15 .

I. INTRODUCTION

Spin-flip scattering of laser light in semiconductors has attracted a great deal of interest in recent years. A number of spin-flip scattering experiments have been carried out with *n*-type semiconductors which allowed the properties of mobile electrons and electrons at shallow donor levels to be studied. These experiments were done with InSb,¹ InAs,² PbTe,³ CdS,⁴⁻⁶ ZnSe,^{5,6} CdTe,⁷ CdSe,⁷ GaAs,⁸ and Hg_xCd_{1-x}Te.⁹ A review of this work has been given by Scott.¹⁰

In contrast to the work with *n*-type materials, there has been only one published report of spin-flip scattering in a *p*-type material, that of spin-flip scattering from holes in ZnTe.^{11,12} The only study prior to that of ZnTe involving hole spin-flip scattering was that of Thomas and Hopfield in 1968,⁴ on holes bound to neutral acceptors in *n*-CdS.

Spin-flip scattering from holes in the valence band of a semiconductor was first considered theoretically by Yafet in 1966.¹³ In this process, the degenerate valence-band energy levels are split apart by the application of a magnetic field. Laser light of energy near the band gap E_G can then cause spin-reversal transitions in the valence band, which proceed via intermediate states in the conduction band. This scattering process and the determination of the valence-band energy-level splittings for the case of ZnTe are considered in a separate paper.¹⁴

For spin-flip scattering from mobile holes a *p*-type semiconductor is required, with the Fermi level in the valence band. The energy gap of *p*-ZnTe at 2 °K (2.391 eV),¹⁵ happens to coincide¹⁶ almost exactly with the energies available from a krypton laser, so this material was a logical choice for study. Hole spin-flip scattering should be observable with almost any *p*-type material, and perhaps *p*-InSb would be another good choice

for future studies.

The purpose of this paper is to present the results of a number of experiments performed on ZnTe. Section II deals with some details of the experimental apparatus and characteristics of the samples. Sections III and IV deal with spin-flip scattering from heavy holes, bound holes, and bound electrons. Several details of the observed spectra are discussed in Sec. V. A simple line-shape model for valence-band spin-flip scattering is presented in Sec. VI. A summary of results and some suggestions for future work are given in Sec. VII.

II. EXPERIMENT

Single crystals of ZnTe were cooled below 2 °K and subjected to steady magnetic fields of up to 148 kG.¹⁷ Laser light was focused into the crystals and the scattered light was collected and analyzed by a double-grating spectrometer and photon-counting system. The samples were illuminated by a krypton laser operating at 5208, 5309, and 5682 Å wavelengths at powers of several hundred mW or less. A cooled RCA C31034A photomultiplier was used for detection. Figure 1 is an isometric view of the superconducting magnet and adjustable sample holder. Microadjustable mirrors were used to translate the laser beam; an external lens and a lens within the helium bath were used to focus the light into a diffraction-limited line within the crystal. Light was collected at 90° from the incident beam and the magnetic field. The horizontal image was rotated to a vertical position and focused onto the entrance slit of the spectrometer after passing through a plane polarizer.

Samples were mounted on pedestals within the sample holder using small amounts of GE7031 varnish. The aluminum sample holder and sample were immersed in the bath of pumped liquid helium. It was assumed that laser heating of the sam-

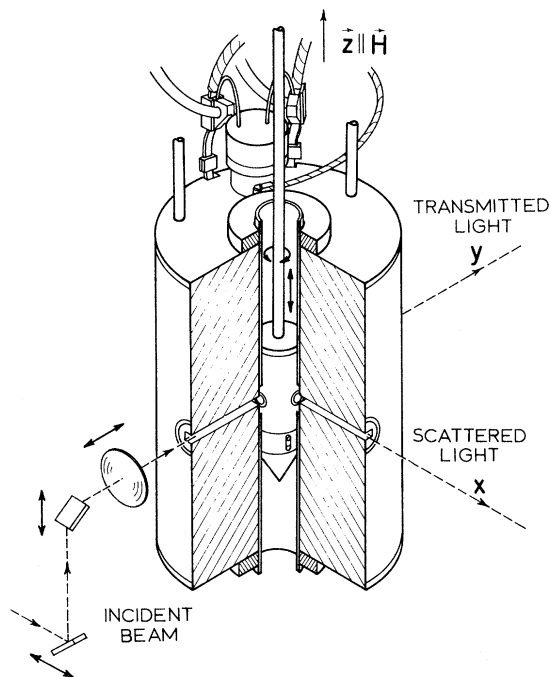


FIG. 1. Superconducting magnet and sample holder. Axes are labeled according to the convention used for the polarization data.

ple was at most a few degrees.

Four different samples of ZnTe were used for this study. All crystals were melt-grown in other laboratories and came with cut and polished faces. None of the crystals were intentionally doped, although upon chemical analysis, crystal ZnTe-1 was found to contain several impurities.¹⁸ It was not possible to analyze the other crystals for impurity content owing to the small amount of material available. The colors of the four crystals varied from dark red to light orange, depending on their purity; samples 2-4 were considerably purer than sample 1. Samples 1 and 2 were analyzed for EPR signals,¹⁹ and transport properties were measured²⁰ down to liquid-nitrogen temperatures for sample 4. Samples 1, 3, and 4 were oriented by using back-scattered Laue photographs; sample 2 was oriented by noting a clear (110) cleavage plane. Table I summarizes the known characteristics of the samples.

As-grown ZnTe is always *p*-type, owing to a natural tendency to form Zn-vacancy acceptor levels.^{21,22} Efforts to produce *n*-type crystals by doping with donor atoms result in highly compensated material with poor electrical properties.²³ An exception²⁴ is Al-doped ZnTe, which is slightly *n*-type; indeed, visible light-emitting *p-n* junction devices have been fabricated.²⁵

TABLE I. Characteristics of ZnTe samples.

Sample: ZnTe-1
Size: $3 \times 4 \times 15 \text{ mm}^3$
Color: Dark red
Origin: Aerospace Research Labs (WPAFB), D. C. Reynolds (Original material from Rocky Mountain Powder Company)
Impurities: Na($\sim 1.5 \times 10^{16}/\text{cm}^3$), In($\sim 2.0 \times 10^{15}/\text{cm}^3$), Ga($\sim 1.0 \times 10^{15}/\text{cm}^3$), Li($\sim 1.0 \times 10^{14}/\text{cm}^3$), Possible trace Cd
Orientation: <i>H</i> is 3.0 deg from [111] direction
EPR: Weak signals at approx. $g=2.06$
Sample: ZnTe-2
Size: $1 \times 2 \times 5 \text{ mm}^3$
Color: Dark orange
Origin: Bell Labs sample No. ZT127 (Harshaw Co.)
Orientation: <i>H</i> is in [100] direction
EPR: No signals
Sample: ZnTe-3 (ARL sample N-5)
Size: $6 \times 5 \times 5 \text{ mm}^3$
Color: Light orange
Origin: Aerospace Research Labs (WPAFB), D. C. Reynolds
Resistivity: $\rho \cong 20 \Omega \text{ cm}$ (300 °K)
Carrier concentration: $n_h \cong 2.7 \times 10^{15}/\text{cm}^3$ (300 °K)
Orientation: <i>H</i> is 16.5 deg from [001] direction in a (100) plane
Sample: ZnTe-4 (ARL sample N-8)
Size: $6 \times 5 \times 5 \text{ mm}^3$
Color: Orange
Origin: Aerospace Research Labs (WPAFB), D. C. Reynolds
Resistivity: $\rho \cong 2.3 \Omega \text{ cm}$ (300 °K)
Carrier concentration: $n_h \cong 2.7 \times 10^{16}/\text{cm}^3$ (300 °K), $\cong 1.0 \times 10^{13}/\text{cm}^3$ (90 °K)
Orientation: <i>H</i> is in [111] direction
Mobility peak: $\mu_h \cong 500 \text{ cm}^2/\text{V sec}$ at $T=120 \text{ °K}$

Since the primary purpose of the present work is to investigate the spin-flip scattering properties of the pure bulk ZnTe, no effort was made to obtain samples with specific dopants. Such investigations on well-characterized doped samples can hopefully be carried out at a later time.

III. SPIN-FLIP SCATTERING FROM HEAVY HOLES

Although none of the samples were intentionally doped, the four samples studied yielded essentially two different spectra. The pure ZnTe samples each gave a single spin-flip line, whereas the relatively less pure sample showed three distinct spin-flip features.

Scattering results from the relatively pure samples (ZnTe-2, 3, 4) will be considered first. Typical intensities ranged from 10^2 counts/sec to 5

$\times 10^3$ counts/sec with laser powers of 100 mW and 30- μ m slit widths. The purest sample, ZnTe-3, yielded a single weak spin-flip peak with 5309 \AA excitation whose full width at half-maximum (FWHM) was approximately 1.0 cm^{-1} at 80 kG and 1.5 cm^{-1} at 130 kG. The peak was observed to shift linearly with magnetic field, with a g value of $g_3 \approx 0.9 \pm 0.2$. Extremely weak scattering at higher g values was also observed. The Stokes-anti-Stokes intensity ratio for the spin-flip peak was at least eight, indicating nearly complete thermalization with the lattice.

Spin-flip scattering from sample 4 (higher-carrier concentration than that of sample 3) was measured from 80 to 130 kG fields. A weak spin-flip peak was observed at $g_4 = 1.1 \pm 0.1$ with a width of approximately 1.2 cm^{-1} (FWHM). The spin-flip feature in sample 4 was seen with both 5309 and 5208 \AA exciting radiation. The fact that the same energy shift is obtained for two different laser wavelengths shows that the feature is not luminescence. As with sample 3, extremely weak unresolved structure was also observed at g values of $g \approx 1.5$ to ≈ 2.5 . No appreciable anti-Stokes scattering was observed with this sample.

Sample 2 yielded a single scattering feature at approximately $g_2 \approx 0.9 \pm 0.1$ with a width of approximately 4.0 cm^{-1} (FWHM). Typical spectra from this sample are shown in Fig. 2. The xy and xz scattering are remarkably intense, with typical count rates of approximately 5×10^3 counts/sec.

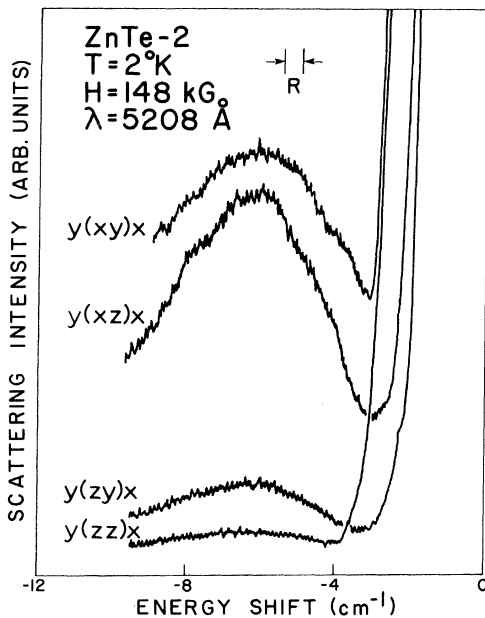


FIG. 2. Spin-flip scattering from pure ZnTe samples. Spectrometer slits are 30 μ m ($\sim 0.5 \text{ cm}^{-1}$ resolution). Laser power is 24 mW.

The spin-flip polarizations varied in character somewhat from sample to sample and will be discussed later.

The g values from the relatively pure samples can be summarized as follows:

$$\vec{H} \parallel [100]: g_3 = 0.9 \pm 0.2, \quad (1)$$

$$\vec{H} \parallel [100]: g_4 = 1.1 \pm 0.1, \quad (2)$$

$$\vec{H} \parallel [100]: g_2 = 0.9 \pm 0.1, \quad (3)$$

listed in order of increasing sample carrier concentration. The intensity of the scattered light increased with increasing carrier concentration, although it was not possible to obtain quantitative comparisons between samples. It is not possible to say with certainty whether the differences in g values between samples is due to anisotropy effects, although the data would indicate larger g values for the $[111]$ direction. Poor signal-to-noise ratios for samples 3 and 4 limited the precision with which g values could be measured.

In order to understand better the nature and origins of the spin-flip transitions, theoretical energy-level calculations were carried out which were appropriate for a p -type semiconductor. The spin-flip scattering is expected to take place between hole levels in the valence band. Spin-flip scattering can also occur from impurity states. The calculations employed the Luttinger-Kohn^{26,27} theory, which has been quite successful in explaining a number of magnetoabsorption results in several materials, but is applied here for the first time to a spin-flip scattering experiment. The details of the calculations are presented in a separate paper.¹⁴ Using this theory, the g values of transitions for the shallowest hole levels are

$$g_{hh}^{av}(2) = 0.92 \pm 0.15, \quad (4)$$

$$g_{hh}^{av}(3) = 2.14 \pm 0.20, \quad (5)$$

$$g_{in}^{av}(0) = 2.33 \pm 0.40, \quad (6)$$

for the two shallowest heavy-hole levels and the shallowest light-hole level. The agreement between the experimental g values g_3 , g_4 , and g_2 and the calculated heavy-hole g value $g_{hh}^{av}(2)$, and the results of a theoretical line-shape calculation (Sec. VI) allow the assignment of the observed scattering features as spin-flip scattering from heavy holes in the ZnTe valence band. This assignment is substantiated by the dependence of spin temperature upon excitation wavelength and by the dependence of scattering intensity upon laser power [to be discussed (Sec. V)].

The theoretical anisotropy is small for the heavy-hole $n=2$ level, resulting in g values of¹⁴

$$\vec{H} \parallel [100]: g_{hh}^{[100]}(2) = 0.88, \quad (7)$$

$$\vec{H} \parallel [111]: g_{hh}^{[111]}(2) = 0.89; \quad (8)$$

approximately 1% larger for the [111] direction but not as large as that suggested by the data.

The (10–15)% discrepancy between theoretical and experimental g values is probably due to the inability of the basic theory to account for such things as exciton effects. Nevertheless, the agreement here is remarkably good. Typical²⁸ band-structure $\vec{k} \cdot \vec{\pi}$ calculations for conduction-electron g values in wide-gap semiconductors show worse agreement with experiment than do the present results.

It is interesting to make further comparisons between the theory and experiment. The additional unresolved scattering between $g \approx 2.5$ agrees roughly with what is expected from $n=3$ heavy-hole and $n=0$ light-hole spin-flip scattering. Scattering from these states is expected to be weak, since they will be populated with fewer holes than the $n=2$ heavy-hole level.

IV. SPIN-FLIP SCATTERING FROM BOUND HOLES AND ELECTRONS

The relatively impure sample, ZnTe-1, yielded in addition to the heavy-hole spin-flip scattering observed in the other samples, two additional lines thought to arise from impurity levels. Figure 3 shows a series of six traces obtained at fields from 40 to 140 kG. At 40 kG, only the laser peak and the rather high luminescent background are discernible. At 60 kG, feature A is becoming visible; at 80 kG, feature B is clearly resolved, and feature C is emerging from the laser line. From 100 to 140 kG, all three features are visible, with a maximum scattering cross section occur-

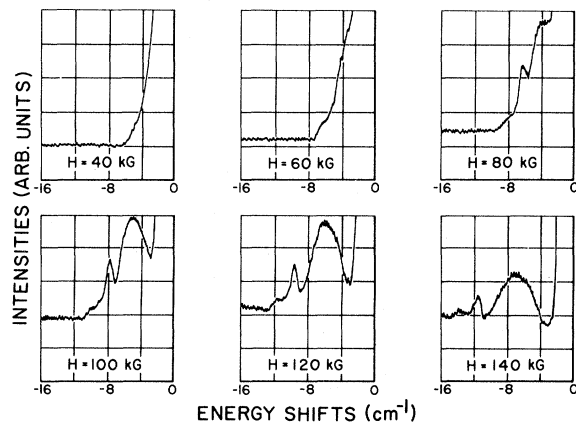


FIG. 3. Spin-flip scattering from relatively impure sample ZnTe-1, at various magnetic fields. Laser excitation wavelength is 5208 Å. Temperature is 1.9°K.

ing at around 100 kG. The luminescent background steadily increases with increasing field owing to the magnetic-field splitting of a nearby shallow bound exciton. The spectra of Fig. 3 dramatically illustrate the necessity of the high fields used for this work.²⁹

Figure 4 shows the magnetic-field dependences of the three spin-flip scattering features. Within the experimental uncertainties, the energy shifts are linear in the field. The g value of C agrees closely with those of the other samples, and is assumed to arise from the heavy-hole spin-flip scattering discussed in Sec. III. Features A , B , and C have measured g values of $g_{1A} = 2.12 \pm 0.04$, $g_{1B} = 1.74 \pm 0.03$, and $g_{1C} \approx 1.07 \pm 0.05$. Features A and B have field-independent widths of approximately 1.0 cm^{-1} (FWHM), and the width of feature C appears to increase with increasing field, being approximately 4.0 cm^{-1} at 130 kG. The marked asymmetry of feature C should be noted.

When sample ZnTe-1 is illuminated with 5309 or 5682 Å laser light, only feature A is observed. Feature A is clearly of entirely different origin than the spin-flip peaks of the purer samples. The ratio of Stokes to anti-Stokes intensities was found to be only 3.2 using 5309 Å light, indicating incomplete thermalization. The spectra at 5682 Å were weaker, and no anti-Stokes peaks were observed.

Figure 5 shows both Stokes and anti-Stokes spin-flip scattering from ZnTe-1 at 5208 Å. The features A , B , and C on the low-energy side of the laser line are riding on top of luminescence from a shallow bound exciton. When this background is subtracted from the total peak heights, the following Stokes–anti-Stokes ratios are ob-

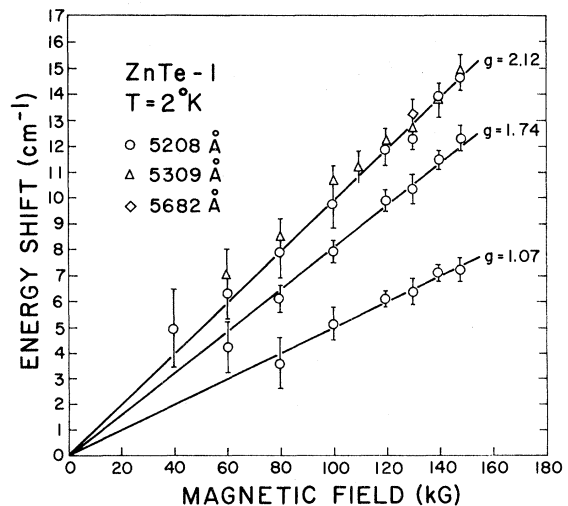


FIG. 4. Energy shift of laser light vs magnetic field for the ZnTe-1 spin-flip scattering features.

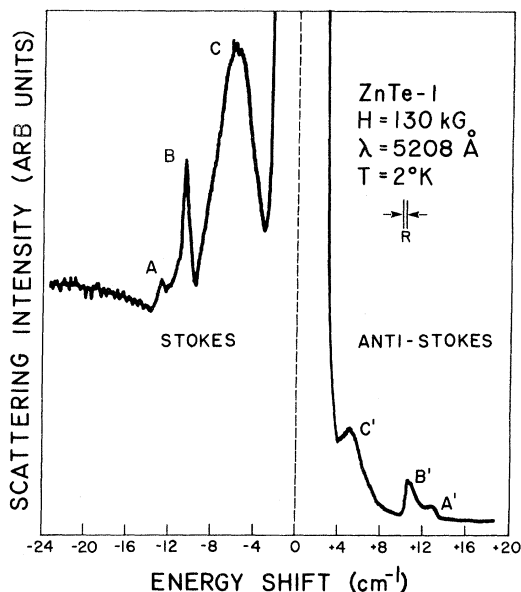


FIG. 5. Stokes and anti-Stokes spin-flip scattering in ZnTe-1.

tained:

$$A/A' \approx 2.0, \quad (9)$$

$$B/B' \approx 4.3, \quad (10)$$

$$C/C' \approx 5.0. \quad (11)$$

These ratios indicate incomplete thermalization of the spin levels with the lattice and will be discussed further in Sec. V.

During the course of several runs it was found that the relative intensities of features *A*, *B*, and *C*, and their anti-Stokes counterparts varied with the laser power. Consequently, a series of runs were made in which the 5208 Å laser power was varied from 10 to 90 mW. The results of these measurements are presented in Fig. 6. Here, the intensities of the three scattering features have been arbitrarily normalized to unity at the maximum power of 90 mW. The intensities of features *B* and *C* increase approximately linearly with laser power, whereas the intensity of *A* increases more rapidly at low power levels and then tends to saturate at the higher laser powers. This behavior indicates that features *B* and *C* are of a different nature than feature *A*.

It should also be mentioned that very weak spin-flip scattering was observed in ZnTe-1 using above band-gap argon laser excitation of 5145 Å. The scattering was essentially the same as that shown in Fig. 3, only more than two orders of magnitude less intense owing to the strong absorption of the 5145 Å radiation by the sample.

The experimental *g* value in ZnTe-1, $g_{1A} = 2.12$

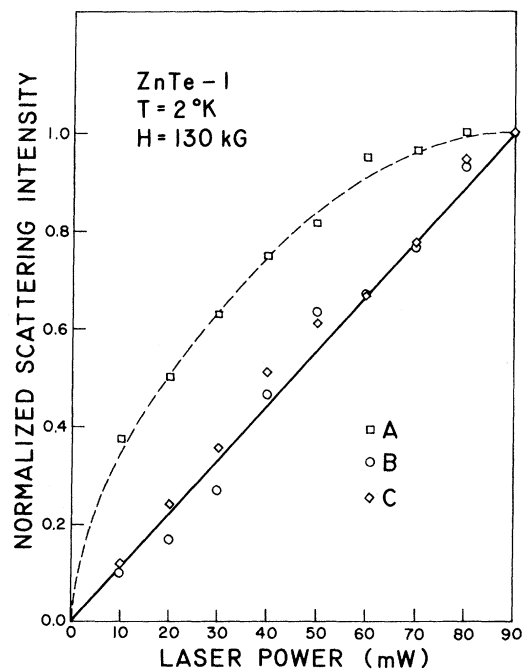


FIG. 6. Scattering intensity vs laser power for the ZnTe-1 spin-flip scattering features. Laser excitation wavelength is 5208 Å.

± 0.04 , is extremely close to the theoretical value $g_{hh}^{av}(3) = 2.14 \pm 0.20$. However, this feature cannot be assigned to $n = 3$ heavy-hole spin-flip scattering¹⁴ for the following reason: The $n = 3$ state is deeper in energy than the $n = 2$ state and therefore will have a lower hole population at our temperatures and photoexcitation levels, consequently, scattering from the $n = 3$ state will only be observable if the $n = 2$ state is also observed. However, in experimental runs at 5309 and 5682 Å (far away from resonance with the band-gap energy E_G), the $g = 2.12$ peak was observed in the absence of an $n = 2$ peak. In addition, the $g = 2.12$ peak was found in only one sample and exhibited a saturation behavior (Fig. 6), unlike that expected for heavy-hole spin-flip scattering. We assign it as spin-flip of a hole trapped at an acceptor level, as discussed below.

When the laser is far away from resonance with the band-gap energy, few holes are photoexcited in the valence band. Although ZnTe is always *p*-type as grown,²¹ the acceptor levels are highly compensated by electrons originating from donor levels near the conduction band. Without photoexcitation, these donor levels will be empty of electrons, the acceptor levels will be partially filled, and the valence band will be completely filled. Spin-flip scattering can then occur from holes in the partially filled acceptor levels. These holes are bound to the impurity ions or lattice vacancies

which give rise to an acceptor level. Whereas the exact nature of the defect center causing the spin-flip scattering is not known, its g value is typical of A centers in II-VI compounds. Title³⁰ has observed EPR from V_{Zn} -Al centers in ZnTe with g values of approximately $g=2.1$.

It is known that ZnTe-1 contains Na and Li impurities which cause acceptor levels to be formed approximately 50 meV above the valence band.²¹ The number of holes available for spin-flip scattering is limited by the number of uncompensated acceptor sites. The saturation behavior of Fig. 6 occurs when the laser light is flipping the spins of essentially all of the bound holes which are available,³¹ and further increases in laser power have little effect, which is not the case for scattering from photoexcited valence-band holes (feature C). Thus there is strong evidence for assigning feature A to spin-flip scattering from bound holes. It should be noted that the weak EPR signals in this sample with $g=2.06$ were obtained without photoexcitation (see Table I).

The remaining scattering peak (feature B in Fig. 5) is not accounted for by theory, nor can it be assigned to bound hole spin-flip scattering since its characteristic dependences are very unlike those of feature A . Its dependence on laser power closely follows that of feature C , which strongly suggests that these two excitations are related. The width of feature B is small (approximately 1.0 cm^{-1} FWHM) and remains constant with field, unlike feature C . The width of B and its behavior are typical⁶ for spin-flip scattering from electrons in wide-gap semiconductors. Since electrons in the conduction band or in donor levels are not subject to the peculiarities of the degenerate valence band, there are no complicated linewidth of line-shape effects, unlike the case for holes in the valence band (see Sec. VI). It therefore seems likely that feature B is due to spin-flip scattering from electrons in donor levels populated by photoexcitation from the laser light.

(The lifetime of *free* electrons is expected to be too short to contribute much to the scattering spectrum.) The g value for such electrons in ZnTe is not known from other work. An early theoretical estimate²⁸ of the conduction-electron g value has yielded a much lower value of $g=0.4$. Shallow donor levels would be expected to have comparable g values.

Sample ZnTe-1 is noteworthy in that spin-flip scattering from bound electrons, bound holes, and valence-band heavy holes are simultaneously observed. The possibility of the simultaneous existence of populated donor and acceptor levels has been discussed by Thomas and Hopfield.⁴

V. DISCUSSION

In this section, details of the spectra are discussed, including the scattering polarizations, photoexcitation of the system by the laser light, and the effective spin temperatures produced by photoexcitation.

A. Polarization

The polarization character of the spin-flip excitation depends on the selection rules in the scattering matrix element. According to Yafet,¹³ the appropriate rule for single-particle spin-flip scattering from both electrons and holes is that

$$\epsilon_{0z}(\epsilon_{1x} - i\epsilon_{1y}) + (\epsilon_{0x} + i\epsilon_{0y})\epsilon_{1z} \neq 0. \quad (12)$$

Here, the ϵ_0 's are the polarizations of the incident light and the ϵ_1 's are the polarizations of the scattered light. The magnetic field is in the z direction. For linearly polarized light, the only allowed polarizations are $y(xz)x$ and $y(zy)x$ in the experimental geometry of Fig. 1. The polarizations $y(zz)x$ and $y(xy)x$ are forbidden.

Experimentally, these rules are obeyed for the case of spin-flip scattering from conduction electrons in CdS,⁵ ZnSe,⁵ and InSb,³² at $5.3 \mu\text{m}$. They do not hold³³ for InSb at $10.6 \mu\text{m}$.

TABLE II. Summary of polarization data.

Wavelength	Polarization	ZnTe-1 (130 kG)	ZnTe-2 (148 kG)	ZnTe-3	ZnTe-4 (130 kG)
5208 Å	zz	0	1	...	0
	zy	1	1	...	1
	xy	1	6	...	1
	xz	10	10	...	10
5309 Å	zz	0	0
	zy	1	0
	xy	0	10
	xz	10	0

The polarization data for the present experiment are summarized in Table II. All data have been corrected for the spectrometer response. The spin-flip intensities are arbitrarily normalized to a scale of 1–10. For 5208 Å, the scattering is predominantly xz in character for the three crystals studied. This is in agreement with theory. However, the weak zy scattering is not in agreement. Also, in ZnTe-2, there is anomalously strong xy scattering. For 5309 Å, ZnTe-4 has large xy scattering, but no xz or zy scattering. The zz scattering component is small for all samples at both wavelengths in accordance with theory. Thus the data clearly suggest a departure from the theory of Yafet, as well as differences among the samples which can only be due to the effects of different impurity levels in the samples.

For conduction electrons in InSb, Patel and Yang³³ obtained strong spin-flip scattering for all polarizations, using 10.6- μm laser radiation. Their observed Landau level transitions also did not follow Yafet's theory. They suggest that collective charge-density fluctuation modes at the spin frequency could account for some zz scattering, but not for their observed xy scattering. They conclude that the zz and xy scattering components in their data cannot be accounted for by a single-particle spin-flip process. They did not investigate the sample dependency of the polarization selection rules.

For spin-flip scattering in CdS and ZnSe, Fleury and Scott⁵ report that the polarization selection rules agree with Yafet's theory. In a later paper,³⁴ however, it is reported that all polarizations become strong when the samples are cooled below about 80 °K.³⁵ They attribute this to entrapment of the conduction electrons at donor sites. It is possible that the anomalous scattering in InSb is also temperature dependent, but temperature studies were not carried out in the experiments of Ref. 33.

In the present experiment, it seems likely that variations in the scattering polarization from sample to sample indicate varying environments for the holes undergoing the spin-flip scattering. Exciton effects cannot be discounted, since the majority of holes in the experiment are produced by photoexcitation.

The possibility of beam depolarization due to the band Voigt effect³⁶ was also considered, but no definite conclusions were reached. This effect becomes divergent as the laser energy approaches the band-gap energy, which is the case in this experiment. Thus small deviations in the polarization of the incident and scattered light from the true x and y directions could lead to elliptically polarized components with nearly random phases.

The presence of impurities differing from sample to sample producing bound exciton levels can also effect the amount of the Voigt phase shift.³⁷

B. Photoexcitation

Holes in the valence band can be produced both thermally and by photoexcitation of the system by the incident laser light. In order to estimate²¹ the thermal population of valence-band holes, one can compute the probability of thermally exciting an electron from the valence band to the lowest known²¹ acceptor level $E_A = 48$ meV in ZnTe at $T = 2$ °K. If this is done, one finds a vanishingly low population of holes in the valence band. Experimentally, from Table I, the measured hole concentration for sample 4 at 90 °K is $n_h \approx 1.0 \times 10^{13}/\text{cm}^3$. The thermal hole population at 2 °K will probably be several orders of magnitude lower than this. Thus the population of thermal holes was quite low at the temperatures at which the experiment was performed.

On the other hand, 100 mW of green laser light corresponds to a photon rate of approximately 3×10^{17} photons/sec. This light was focused into a volume of perhaps 10^{-3} cm³ inside the samples. Since the energy of the laser light is very nearly equal to the band-gap energy E_G , the cross section for hole-electron pair production can be quite high, say, 10% efficiency. Thus approximately 10^{20} to 10^{21} pairs/cm³/sec are produced in the region of interest. The presence of electron trapping levels within the energy gap with lifetimes of the order of 10^{-5} sec can result in steady-state populations of valence-band holes of $n_h \approx 10^{15}/\text{cm}^3$ to $10^{16}/\text{cm}^3$, or perhaps five or six orders of magnitude greater than the population of thermal holes.

The photoexcitation process is illustrated schematically in Fig. 7. In this manner, long-lived hole states are created in the valence band.

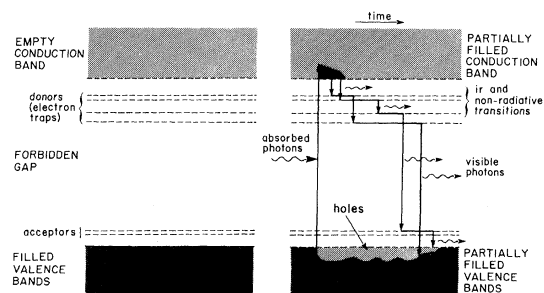


FIG. 7. Photoexcitation process. (Left) with no light on the sample, the valence band is completely filled with electrons. (Right) with laser excitation, long-lived hole states are created in the valence band by the action of trapping levels in the gap.

These holes can then undergo spin-flip scattering by the laser light. Electrons held up in the various trapping levels can also undergo spin-flip scattering. This scattering is observable if the lifetime of a given state is long enough to prevent excessive broadening of the spin levels. Bound electron spin-flip scattering (such as feature *B* in sample 1) is thus seen to occur from some donor level with a lifetime of 10^{-6} sec or longer. Such processes could also contribute to the unresolved scattering from $g \approx 1.5$ to ≈ 2.5 sample 4.

By the model of Fig. 7, impurity type and concentration can directly influence the number of valence-band holes available, and hence the spin-flip scattering intensity. The data are in qualitative agreement with this model, since the observed intensities increase with increasing impurity concentrations. It is to be emphasized that the impurity levels themselves need not be directly involved in the heavy-hole spin-flip scattering, but do provide a mechanism for the photoproduction of holes in the valence band, which can then undergo spin-flip scattering. It is not possible at this time to make further quantitative estimates without well-characterized samples with known impurity types and concentrations. The actual presence of specific impurity levels in the samples was studied by means of luminescence from bound exciton levels. Analyses of the Zeeman splitting of extremely shallow bound excitons gave hole g values compatible with the heavy-hole spin-flip results.³⁸

C. Spin temperature

For the pure samples of ZnTe, almost no anti-Stokes scattering was observed, indicating that the spin system was in thermal equilibrium with the lattice.

For ZnTe-1, which contained several impurities, small values of the Stokes-anti-Stokes ratio were found when the laser light approached resonance with the band gap. If a simple two-level system with spins α and β is assumed, and the viewpoint is taken that the energies E_α and E_β represent the total energies of all the spins in states α and β , and further that some mechanism exists which allows the two spin systems to equilibrate with each other, then an effective spin temperature can be computed from the Boltzmann factor relating the populations of the two levels.³⁹ The results for ZnTe-1 are given in Table III. Here, the effective spin temperature is given for each scattering feature at the three wavelengths used. (Features *B* and *C* were only observable with 5208 or 5145 Å exciting radiation.)

The results for feature *A* (bound-hole spin flip) are particularly interesting. Far away from reso-

TABLE III. Effective spin temperatures for ZnTe-1.

Wavelength	Feature		
	<i>A</i> ($g=2.12$)	<i>B</i> ($g=1.74$)	<i>C</i> ($g=1.07$)
5208 Å	27 °K	10 °K	6 °K
5309 Å	16 °K
5682 Å	1.8 °K

(Lattice temperature = 1.8 °K)

nance, the spin systems and the lattice are in thermal equilibrium with each other and with the bath of pumped liquid helium (1.8 °K). As the laser energy approaches the band-gap energy, the scattering intensity increases in accordance with a resonant denominator, a large number of electron-hole pairs are produced by photoexcitation, and the upper spin level of the acceptor state becomes excessively populated, raising the effective spin temperature. The rate at which the upper spin level spontaneously decays into the lower spin level is limited by the spin-lattice relaxation time.

At 5208 Å, features *B* and *C* also have elevated spin temperatures, although not as much as feature *A*. It should be remarked that for n -CdS, Thomas and Hopfield⁴ found that their bound-electron spin flip showed incomplete thermalization even at very low laser powers, whereas the bound-hole spin flip showed complete thermalization. They concluded that the spin-orbit coupling in the valence band results in a much stronger coupling of the holes to the lattice than for the bound electrons.

VI. SIMPLE LINE-SHAPE MODEL

All possible transitions between the various valence-band levels are allowed in the Raman effect.⁴⁰ Thus, in principle, one should be able to observe transitions between principal quantum levels (Landau level scattering)¹; transitions from the light- to heavy-hole bands and vice versa; transitions in which the spin is flipped and the Landau level is changed,¹ and finally, pure spin-flip transitions where the principal quantum number n remains unchanged. This plethora of scattering effects is not observed for the following reason: Mobilities in II-VI semiconductors are usually poor, and at low temperatures are restricted by screened ionized impurity scattering.⁴¹ Even at high-field values, $\omega_c \tau$ is much less than unity, where ω_c is the cyclotron resonance frequency and τ is the collision lifetime. Thus, for example, in sample ZnTe-4, even the measured peak mobility of 500 cm²/V sec at 120 °K will re-

sult in "smeared-out" Landau levels. In this case, the collision lifetime is much shorter than the time required for a hole to execute a single cyclotron orbit. On the other hand, the spin-lattice relaxation time may be 10^6 times greater than the collision time.⁴² This fact, along with the effects of motional narrowing,⁴³ result in well-defined spin levels. Thus we expect to observe sharp spin-flip lines, and only broad, unresolved Landau level lines. Of the many possible spin-flip transitions, most will be excluded by the Pauli principle at the temperatures and photoexcitation levels of our experiments.

There have been a number^{32,44-47} of theoretical investigations of the spin-flip line shape in the narrow gap material n -InSb. The considerations of these papers are not wholly applicable to the present case of spin-flip scattering in the ZnTe valence band. In n -InSb spin-flip scattering, there are no valence-band complications; it is necessary only to consider the quantum limit case at $T = 0$, and the collision time is generally^{32,44} considered to be independent of the field. The small band gap and large g value in InSb do, however, make the spin-flip linewidth and line shape more dependent upon field and excitation wavelength than in ZnTe.

A complete microscopic theory of the spin-flip line shape in ZnTe will not be presented here. Instead, a simple theoretical model is discussed, which accounts for most of the observed line-shape effects.

The basic spin-flip lineshape in the absence of k_H -dependent effects is assumed to have a simple Lorentzian form whose width is a function of the magnetic field:

$$\Gamma = a + bH + O(H^2) + \dots, \quad (13)$$

where a and b are material-dependent and temperature-dependent constants. The fundamental dependences of a and b on these parameters depend on the formulation of the exact theory. The term a is expected to increase with increasing temperature and effective carrier concentrations. The work by Auyang⁴⁶ (S. Y. Yuen) on the spin-flip linewidth in InSb includes these dependences as part of her basic diffusion theory.

The second term in Eq. (13) arises from the assumption that scattering from screened ionized impurities is the dominant process limiting the hole lifetimes. The magnetic field tends to "stretch out" the impurity wave functions along the field direction, decreasing their cross sections for scattering holes. Also, the cyclotron orbit radii of holes decrease with increasing field, limiting the number of collisions. Because of motional narrowing, the spin-flip linewidth will increase with increasing collision time. Motional

narrowing occurs because an increase in the collision frequency results in an increase in the fluctuation frequency of local magnetic fields seen by the individual spins. This tends to inhibit dephasing of spins in a group of spins which starts out in phase with each other. Argyres and Adams⁴⁸ have shown that the collision time varies approximately linearly with the magnetic field. The constant b will depend on the screening length of the ionized impurities, and will not be evaluated here.

The more important contributions to the spin-flip line shape in ZnTe arise not from the form of Γ , but from the k_H dependence of the energy levels (see Ref. 14). Thus, considering the shallowest heavy-hole level ($n=2$), the spin-flip line for a fixed value of k_H will have the complex form

$$G(\omega, k_H) = \frac{1}{\omega - \omega_s(k_H) - i\Gamma/2}, \quad (14)$$

where Γ is given by Eq. (13) and the spin-flip frequency $\omega_s(k_H)$ is given by

$$\omega_s(k_H) = |\epsilon_\alpha^-(k_H) - \epsilon_\beta^-(k_H)|_{(n=2)}. \quad (15)$$

where $\epsilon_\alpha^-(k_H)$ and $\epsilon_\beta^-(k_H)$ are the energies of the spin-split $n=2$ heavy-hole level. The resulting spectrum will contain contributions from all values of k_H , weighted by the appropriate probability factor. As we have seen, the presence of photoexcitation processes results in high effective spin temperatures and limits the utility of describing the system in terms of Fermi statistics, since the spins are not in thermal equilibrium with the lattice. If it is assumed, however, that Fermi statistics are approximately valid at low effective spin temperatures, then the joint probability that the lower spin level is occupied by a hole for a given value of k_H is

$$f(k_H) = \begin{cases} (1-f_\beta)f_\alpha, & \epsilon_\alpha > \epsilon_\beta, \\ (1-f_\alpha)f_\beta, & \epsilon_\beta > \epsilon_\alpha \end{cases}, \quad (16)$$

where

$$f_\alpha = \frac{1}{\exp\{[E_F - \epsilon_\alpha^-(k_H)]/k_B T\} + 1} \quad (17)$$

and

$$f_\beta = \frac{1}{\exp\{[E_F - \epsilon_\beta^-(k_H)]/k_B T\} + 1}. \quad (18)$$

Combining Eq. (16) with Eq. (14) and integrating over k_H , the spectral line shape results:

$$S(\omega) = \text{Im} \int_0^\infty G(\omega, k_H) f(k_H) dk_H. \quad (19)$$

The finite width of $G(\omega, k_H)$ serves to account approximately for the rounding-off of the density of states near $k_H = 0$.⁴⁹

Figure 8 shows the results of numerical calcu-

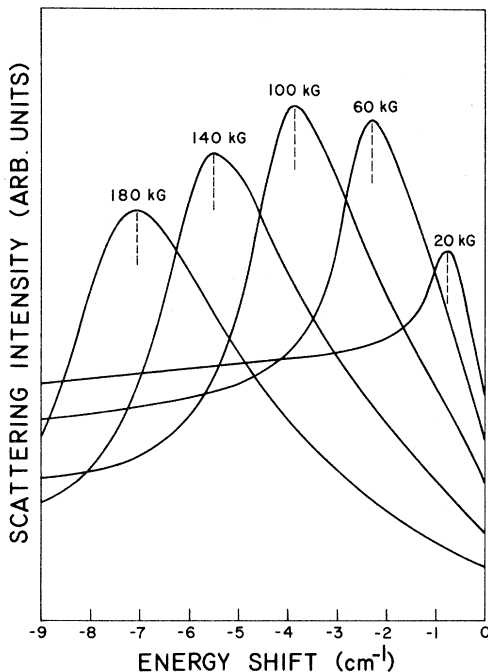


FIG. 8. Theoretical heavy-hole spin-flip line shape in ZnTe at various magnetic fields.

lations using Eq. (19), for various values of the magnetic field. Values of $a = 0.8 \text{ cm}^{-1}$, $b = 1 \times 10^{-5} \text{ cm}^{-1}/\text{G}$, $E_F = 2.0 \text{ cm}^{-1}$, and $T = 2.0 \text{ }^\circ\text{K}$ were used for the plot. The spin-flip line shape is highly asymmetric, with a tail on the low-energy side of the peak. The position of the peak is negligibly shifted from the nominal $k_H = 0$ frequency. A maximum peak height is reached at around $H = 100 \text{ kG}$ and then falls off at increasing fields, although at high fields the integrated cross section remains approximately constant. The theoretical curve at $H = 20 \text{ kG}$ was not observable in the experiment due to strong Rayleigh scattering, and the 180 kG curve is above the capabilities of the magnet. The remaining curves are to be compared with the experimental results on feature C in Fig. 3. Agreement between the theoretical model and the experiment is quite good, although detailed comparison is hampered by the width of the laser line and the magnetic-field effects on the bound exciton luminescence in the experimental traces.

The model is capable of predicting several effects, the details of which will not be presented here. For example, a linewidth which increases with increasing impurity concentration is predicted. This arises partly from the a term in Eq. (13) and partly from an increase in the Fermi energy E_F due to increased carriers. The effect is in qualitative agreement with experiment. The model also predicts a linewidth which increases

with increasing temperature. Unfortunately, the experimental arrangement did not allow for variation of the temperature. An interesting prediction due to the k_H dependency is that the Stokes and anti-Stokes peaks need not appear equidistant from the laser line. The anti-Stokes peak will lie a few tenths of a wave number closer to the laser line than the Stokes peak. This effect was observed in several experimental runs (see Fig. 5). Other Raman studies of broad features have shown similar effects.⁵⁰

The theoretical model, although incomplete, does provide general agreement with experiment. It is hoped that this work will at least inspire the development of a microscopic theory in the near future.

VII. CONCLUDING REMARKS

This paper considerably expands on the first experimental observation of spin-flip scattering in ZnTe reported by us in 1973.¹¹ This was the first spin-flip scattering experiment to be performed in a p -type material. The main result has been the identification of spin-flip scattering from valence-band hole states (heavy holes), predicted theoretically by Yafet in 1966.¹³ Whereas the detailed assignments of Ref. 11 have been modified by further experimental and theoretical work since 1973, the overall interpretation remains substantially correct. Measured heavy-hole g values for ZnTe varied from $g \approx 0.9$ to ≈ 1.1 depending on the sample. In addition to some measurement uncertainties, the variation in g value is thought to originate partly from exciton effects. It is also possible that small amounts of strain were inadvertently introduced to the samples, which should slightly affect the g values.

Spin-flip scattering from impurity states was also observed. These scattering features behaved differently in several ways from the heavy-hole scattering and were not accounted for by theory. A bound hole g value of $g = 2.12$ and a bound electron with $g = 1.74$ were observed in one of the samples. The bound hole g value agrees with those of other measurements.³⁰ The g value for electrons in ZnTe is unknown from other work, so this appears to be the first determination of an electron g value in ZnTe. The scattering state is thought to be that of a shallow donor, but the g value should approximate that of the conduction electrons. The present experiment is also the first spin-flip scattering from photoexcited states in a semiconductor.

In the course of the spin-flip work, a new second-order light scattering process was discovered which gives line spectra at $-\omega_{\text{LO}} \pm \omega_{\text{SF}}$, where ω_{LO}

is a longitudinal-optical phonon frequency and ω_{SF} is a hole or electron spin-flip frequency. This scattering is only present when the excitation energy is greater than the band gap energy. This effect was reported previously¹² and will not be discussed here.

It is perhaps appropriate to compare the technique of spin-flip scattering with that of electron paramagnetic resonance (EPR).⁵¹ Title³⁰ has explained the difficulty of using EPR to measure g values for mobile holes in zinc-blende structures: Small random strains produce splittings which vary across the sample; the EPR signal is consequently smeared out beyond detectability limits. Spin-flip scattering is not severely affected by this broadening; indeed, transitions 4 cm^{-1} wide are shown in Fig. 2. These could not be detected by conventional EPR techniques. Furthermore, intense photoexcitation is required to produce observable hole populations—a requirement difficult to satisfy with conventional EPR equipment. We believe that spin-flip scattering of laser light can be a power-

ful new tool for investigating the valence-band structure of semiconductors as well as the magnetic properties of defect complexes.

Possible extensions of the present work include varying the temperature, varying the geometry, and applying uniaxial stress to the sample. Stimulated scattering should be possible if enough input power is available.⁵² The magnetic properties of bound states could be studied by resonant spin-flip scattering techniques employing a dye laser. Outstanding theoretical problems also remain.

ACKNOWLEDGMENTS

It is a pleasure to acknowledge the active collaboration with J. F. Ryan and D. J. Toms in the early experiments, and to thank Elizabeth Cawthra Hollis for assistance in taking the data. Communications with several persons proved helpful during the course of the work. In particular, communications with P. A. Wolff and R. A. Stradling are gratefully acknowledged.

*Work supported by NSF Grant No. GH-34681, by the U. S. Air Force, contract F33615-74-C-4018 (Aerospace Research Laboratories, Wright-Patterson AFB), and by AFOSR Grant No. 75-2835.

†Present address: NSF-CNRS Exchange Scientist, Université Pierre et Marie Curie, Paris, France.

¹R. E. Slusher, C. K. N. Patel, and P. A. Fleury, *Phys. Rev. Lett.* **18**, 77 (1967).

²C. K. N. Patel and R. E. Slusher, *Phys. Rev.* **167**, 413 (1968).

³C. K. N. Patel and R. E. Slusher, *Phys. Rev.* **177**, 1200 (1969).

⁴D. G. Thomas and J. J. Hopfield, *Phys. Rev.* **175**, 1021 (1968).

⁵P. A. Fleury and J. F. Scott, *Phys. Rev. B* **3**, 1979 (1971).

⁶J. F. Scott, T. C. Damen, and P. A. Fleury, *Phys. Rev. B* **6**, 3856 (1972).

⁷T. W. Walker, C. W. Litton, D. C. Reynolds, T. C. Collins, W. A. Wallace, J. H. Gorrell, and K. C. Jungling, *Proceedings of the Eleventh International Conference on the Physics of Semiconductors* (PWN-Polish Scientific, Warsaw, 1972).

⁸T. W. Walker, T. F. Deaton, J. H. Gorrell, C. W. Litton, D. C. Reynolds, T. C. Collins, and W. A. Wallace, *Bull. Am. Phys. Soc.* **18**, 300 (1973).

⁹J. P. Sattler, B. A. Weber, and J. Nemanich, *Appl. Phys. Lett.* **25**, 491 (1974).

¹⁰J. F. Scott, in *Physics of Quantum Electronics 2*, edited by S. F. Jacobs, M. Sargent III, J. F. Scott, and M. O. Scully (Addison-Wesley, Reading, Mass., 1975), p. 123.

¹¹R. L. Hollis, J. F. Ryan, D. J. Toms, and J. F. Scott, *Phys. Rev. Lett.* **31**, 1004 (1973).

¹²R. L. Hollis, J. F. Ryan, and J. F. Scott, *Phys. Rev. Lett.* **34**, 209 (1975).

¹³Y. Yafet, *Phys. Rev.* **152**, 858 (1966).

¹⁴R. L. Hollis, preceding paper, *Phys. Rev. B* **15**, 932 (1977).

¹⁵A. C. Aten, C. F. Van Doorn, and A. T. Vink, in *Proceedings of the International Conference on the Physics of Semiconductors, Exeter, 1962*, edited by A. C. Strickland (Institute of Physics and the Physical Society, London, 1962), p. 696.

¹⁶This fact was pointed out by C. W. Litton who had achieved some preliminary results with this material (private communication).

¹⁷For additional details of the experimental apparatus, refer to R. L. Hollis, Ph.D. thesis (Univ. of Colorado, 1975) (unpublished) (University Microfilms, Ann Arbor, Mich.).

¹⁸Analysis done by Eagle-Picher Industries, Inc., Miami Research Laboratories, P. O. Box 1090, Miami, Okla. 74354, on samples from the same boule supplied by C. W. Litton.

¹⁹This work was done by G. Troeger and R. Yeats.

²⁰This work was done by J. Sites and H. Washburn.

²¹M. Aven and B. Segall, *Phys. Rev.* **130**, 81 (1963).

²²D. G. Thomas and E. A. Sadowski, *J. Phys. Chem. Solids* **25**, 395 (1964).

²³A. G. Fischer, J. N. Carides, and J. Dresner, *Solid State Commun.* **2**, 157 (1964).

²⁴F. T. J. Smith, *Solid State Commun.* **9**, 957 (1971).

²⁵J. Marine, Abstract for IEEE Conference on Luminous Devices, Atlanta (1974) (unpublished).

²⁶J. M. Luttinger and W. Kohn, *Phys. Rev.* **97**, 869 (1955).

²⁷J. M. Luttinger, *Phys. Rev.* **102**, 1030 (1956).

²⁸See, for example, M. Cardona, *J. Phys. Chem. Solids* **24**, 1543 (1963).

²⁹R. L. Hollis, J. F. Ryan, and W. J. O'Sullivan, *Cryogenics* **14**, 8 (1974).

³⁰R. S. Title, in *Physics and Chemistry of II-IV Compounds*, edited by M. Aven and J. S. Prener (North

Holland, Amsterdam, 1967), p. 304.

³¹Y. R. Shen has informed us of similar saturation effects at such low power levels for impurity scattering processes in other crystals (private communication).

³²S. R. J. Brueck, A. Mooradian, and F. A. Blum, *Phys. Rev. B* **7**, 5253 (1973).

³³C. K. N. Patel and K. H. Yang, *Appl. Phys. Lett.* **18**, 491 (1971).

³⁴J. F. Scott, in *Advances in Raman Spectroscopy, Vol. I, Proceedings of the Third International Conference on Raman Spectroscopy, Reims, 1972*, edited by J. P. Mathieu (Heyden and Son, London, 1973), p. 353.

³⁵Recent experiments, however, on one sample of ZnSe indicate that Yafet's selection rules are obeyed at 2°K R. L. Hollis (unpublished).

³⁶S. Teitler and E. D. Palik, *Phys. Rev. Lett.* **5**, 546 (1960).

³⁷R. F. Wallis and D. L. Mitchell (unpublished) cited by L. M. Roth, *Phys. Rev.* **133** A, 542 (1964).

³⁸R. L. Hollis and J. F. Scott, *Bull. Am. Phys. Soc.* **20**, 363 (1975); see also Ref. 17, and *Solid State Commun.* (in press).

³⁹For a discussion of the concept of spin temperature for a number of situations, see A. Abragam and W. G. Proctor, *Phys. Rev.* **109**, 1441 (1958).

⁴⁰See, for example, H. J. Zeiger and G. W. Pratt, *Magnetic Interactions in Solids* (Oxford U.P., London, 1973), p. 392.

⁴¹See, for example, S. S. Devlin, in *Physics and Chemistry of II-VI Compounds*, edited by M. Aven and J. S. Prener (North Holland, Amsterdam, 1967), p. 567.

⁴²For a theoretical treatment, see Y. Yafet, in *Solid State Phys.* **14**, 1 (1963).

⁴³See, for example, C. P. Slichter, *Principles of Magnetic Resonance* (Harper and Row, New York, 1963), p. 115.

⁴⁴S. R. J. Brueck, Ph.D. thesis (M.I.T., 1971) (unpublished).

⁴⁵R. W. Davies, *Phys. Rev. B* **7**, 373 (1973).

⁴⁶Y. C. S. Auyang (S. Y. Yuen), Ph.D. thesis (M.I.T., 1971) (unpublished).

⁴⁷S. Y. Yuen, P. A. Wolff, and B. Lax, *Phys. Rev. B* **9**, 3394 (1974).

⁴⁸P. N. Argyres and E. D. Adams, *Phys. Rev.* **104**, 900 (1956).

⁴⁹For a more accurate approach to taking into account the density of states function, see Ref. 47.

⁵⁰P. S. Peercy, *Phys. Rev. Lett.* **31**, 379 (1973).

⁵¹J. F. Scott, R. L. Hollis, D. L. Fox, C. A. Helms, R. W. Kinne, and J. F. Ryan, in *Light Scattering in Solids, Proceedings of the Third International Conference on Light Scattering in Solids, Campinas, 1975* (Flammarion, Paris, 1976), p. 224.

⁵²Stimulated spin-flip scattering has been achieved in the wide-gap semiconductor CdS. See J. F. Scott and T. C. Damen, *Phys. Rev. Lett.* **29**, 107 (1972).